



Cite this: DOI: 10.1039/c7dt02387a

# A long-range emissive mega-Stokes inorganic–organic hybrid material with peripheral carboxyl functionality for As(v) recognition and its application in bioimaging†

M. Venkateswarulu,<sup>a</sup> Diksha Gambhir,<sup>a</sup> Harpreet Kaur,<sup>a</sup> P. Vineeth Daniel,<sup>a</sup> Prosenjit Mondal<sup>a</sup> and Rik Rani Koner<sup>\*b</sup>

We demonstrate a strategy for the recognition of As<sup>5+</sup> in aqueous solution using a red-emissive probe based on a perylene–Cu<sup>2+</sup> ensemble decorated with peripheral free carboxyl functionality. Single crystal analysis helped us to understand the chemical structure of the probe. To the best of our knowledge, this is the first probe for arsenic detection which emits in the red region ( $\lambda_{em} = 600$  nm). The perylene–Cu<sup>2+</sup> ensemble exhibited a mega-Stokes shift (>100 nm) with a high degree of selectivity upon interaction with As<sup>5+</sup>, which indicated that the present probe has the potential to be used as a turn-on optical sensor for selective detection of As<sup>5+</sup> with fewer experimental limitations. The detection limit was found to be 26 nM. Inspired by its good emissive properties, the ensemble was further explored for imaging As<sup>5+</sup> in live cells. Because of its long-range emissive nature, no autofluorescence from the cellular species was observed during the imaging process. The probe was evaluated to be non-toxic and successfully permeated the cell membrane without the help of any permeabilizing agent to image As<sup>5+</sup>.

Received 2nd July 2017,  
Accepted 30th August 2017

DOI: 10.1039/c7dt02387a

rsc.li/dalton

## Introduction

Among the various factors responsible for water pollution, arsenic contamination is a global concern.<sup>1,2</sup> Substantial efforts are being devoted by scientists and engineers toward the development of different tools for arsenic detection<sup>3–5</sup> and innovative technologies for its separation and removal.<sup>6–9</sup>

Arsenic is a highly toxic metalloid which is ubiquitous in natural water resources. Leaching of arsenic containing rocks into the aquifers is mainly responsible for the contamination.<sup>2</sup> Due to its high toxicity, arsenic has been classified as a group 1 human carcinogen by the International Agency for Research on Cancer.<sup>10</sup> Arsenic exists in four different oxidation states (–3, 0, +3, +5) of which the two toxic inorganic forms, namely, arsenate (+5) and arsenite (+3), are usually found in water.<sup>11</sup> Prolonged exposure to even low levels of arsenic causes various

cardiovascular disorders such as atherosclerosis, hypertension, ischemic heart diseases and ventricular arrhythmias.<sup>2,12–15</sup> The maximum permissible limit of arsenic in drinking water as recommended by the World Health Organization (WHO) is 10  $\mu\text{g L}^{-1}$ .<sup>16</sup>

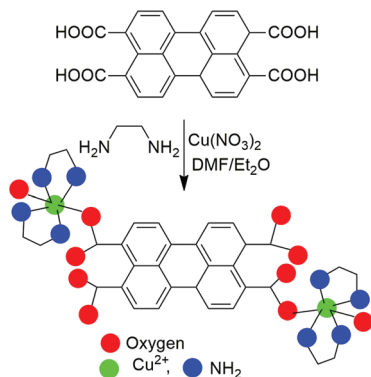
Many conventional analytical techniques are often used to sense arsenic, such as atomic fluorescence spectroscopy (AFS),<sup>17–19</sup> cathodic stripping voltammetry (CSV) using a hanging drop mercury electrode,<sup>20</sup> anodic stripping voltammetry (ASV),<sup>21–24</sup> hydride generative inductively coupled plasma atomic emission spectrometry (HG-ICP-AES),<sup>25</sup> etc. However, many of these techniques are not effective from an economical point of view and involve complex operational procedures although they offer very low detection limits. In this regard, in recent times, absorption and fluorescence spectroscopy methods have been explored for efficient and quick detection of different forms of arsenic, particularly As<sup>3+</sup> and As<sup>5+</sup> using innovatively designed new optical materials.<sup>8,26–29</sup> Very recently, metal–organic ensembles have been reported to be highly promising emissive materials for detection of arsenic derivatives at very low concentration.<sup>30,31</sup>

As the arsenic pollution causes several health disorders, fluorescent probes for its detection are gaining much attention from researchers as these probes can be utilized for optical imaging of arsenic in biological systems.<sup>28,29,32</sup> Hence, as a

<sup>a</sup>School of Basic Sciences, Indian Institute of Technology Mandi, Mandi-175001, H.P., India

<sup>b</sup>School of Engineering, Indian Institute of Technology Mandi, Mandi-175001, H.P., India. E-mail: rik@iitmandi.ac.in; Fax: +91 1905 237924; Tel: +91 1905 267220

† Electronic supplementary information (ESI) available. CCDC 1559082. For ESI and crystallographic data in CIF or other electronic format see DOI: 10.1039/c7dt02387a. This crystal structure was previously reported by Y. Suenaga *et al.*, Polyhedron, 1998, 17, 2207, DOI: [http://dx.doi.org/10.1016/S0277-5387\(98\)00043-6](http://dx.doi.org/10.1016/S0277-5387(98)00043-6) [ref. 45(b)].



**Scheme 1** The synthetic route for the PTCA-Cu<sup>2+</sup> complex.

long-standing need in fluorescence microscopy, emissive probes with long wavelength emission properties are always desirable due to reduced photon scattering and the possibility to obtain sharp contrast images.

In addition, emissive probes with a mega-Stokes shift are more desirable as they substantially reduce experimental limitations including self-absorption, interference from light sources *etc.*<sup>33,34</sup> To our knowledge, the largest emissive small molecule probe that has been reported so far (Table S1<sup>†</sup>) for arsenic imaging emits in the green region ( $\lambda_{em} = 552 \text{ nm}$ ).<sup>35</sup>

In this context, As<sup>5+</sup> recognition using a perylene-Cu<sup>2+</sup> ensemble decorated with peripheral carboxyl functionality as a mega-Stokes red-emissive ( $\lambda_{em} = 600 \text{ nm}$ ) probe has been successfully achieved. To the best of our knowledge, this is the first red-emissive small molecule probe for arsenic recognition to be reported so far. The probe permeates the cell membrane easily without any permeabilizing agent and images As<sup>5+</sup> inside live cells with no background fluorescence issue.

The carboxylic acid functionalized perylene moiety (H<sub>4</sub>PTCA) served as a ligand for the stabilization of Cu<sup>2+</sup> in the presence of ethylenediamine. The PTCA-Cu<sup>2+</sup> platform was synthesized following an easy accessible synthetic method and fully characterized using various analytical techniques such as FT-IR, NMR, HRMS and SCXRD (Fig. S1–S5<sup>†</sup>). This integrated system of Cu<sup>2+</sup> linked with a carboxyl group decorated perylene moiety was investigated (Scheme 1) as an optical tool for the detection of As<sup>5+</sup> in an aqueous medium in the presence of several cations and anions. Various spectroscopic techniques have been employed to evaluate the selective affinity of PTCA-Cu<sup>2+</sup> towards As<sup>5+</sup>.

## Experimental methods and materials

### Materials and instruments

All reagents and solvents were purchased from Alfa Aesar and Sigma-Aldrich. Freshly prepared standard solutions of tetrabutylammonium salts of all anions and nitrate salts of all cations (1 mM) in deionized (DI) H<sub>2</sub>O buffered with HEPES (1 mM), pH = 7.2, were used for UV-vis and fluo-

rescence spectral studies. PerkinElmer Spectrum 2 spectrophotometer was used to record FT-IR spectra. Jeol-ECX-500 MHz spectrometer (tetramethylsilane as an internal standard) was used to record <sup>1</sup>H and <sup>13</sup>C NMR spectra in D<sub>2</sub>O-*d*<sub>2</sub>. Bruker impact-HD spectrometer (quadrupole-time-of-flight mass analyser) was used to record HRMS spectra. SHIMADZU UV-2450 spectrophotometer and Cary Eclipse spectrophotometer were used to record absorption and fluorescence spectra respectively.

### Single-crystal X-ray diffraction studies (SCXRD)

A suitable single crystal of PTCA-Cu<sup>2+</sup> complex was grown in a glass tube by slow diffusion method for X-ray diffraction analysis. The SCXRD data of the complex were recorded using Cu K $\alpha$ ,  $\lambda = 1.5406 \text{ \AA}$  at 298(2) K source in Agilent Technologies X-ray diffractometer system. The SCXRD data revealed that the PTCA-Cu<sup>2+</sup> complex crystallized in monoclinic crystals with the *P21/c* space group. CrysAlisPro' Software (online version) was used for data collection and CrysAlisPro' Software (offline version)<sup>36</sup> was used for data reduction. The structure of the complex was solved using OLEX<sup>2</sup> software and the full-matrix least-squares ( $F^2$ ) method in SHELXL-97<sup>37,38</sup> was used for structure refinement. All hydrogen atoms were obtained after refined anisotropically located non-hydrogen atoms. The detailed complex crystal structure parameters have been given in Table S2.<sup>†</sup>

### UV-vis and fluorescence titrations

UV-vis and fluorescence experiments were performed in H<sub>2</sub>O buffered with HEPES (1 mM, pH = 7.2). All fluorescence titrations were performed using a 10  $\mu\text{M}$  complex/ligand solution and a 1 mM solution of anions/cations. The fluorescence excitation and emission wavelengths were 497 nm and 600 nm with 5/10 slit widths, respectively. For every titration, 3 mL of a freshly prepared 10  $\mu\text{M}$  complex/ligand solution was taken in a 3.5 mL quartz cuvette (path length 1 cm), and titrated with the desired amount of anions/cations. The stock solutions of complex/ligand and all anions/cations for UV-vis and fluorescence titrations were used in high concentrations to avoid dilution errors.

### DFT calculations

Additionally, the geometries of the ligand (H<sub>4</sub>PTCA) its copper complex (PTCA-Cu<sup>2+</sup>) and ensemble with arsenate (PTCA-As<sup>5+</sup>) were optimized with the help of density functional theory (DFT) using the B3LYP/6-31G(d,p) basis set<sup>39,40</sup> for the ligand and PTCA-As<sup>5+</sup> system. Similarly, the B3LYP/LANL2DZ basis set was used for PTCA-Cu<sup>2+</sup> with no symmetry constraints using the Gaussian 09 suite of programs.<sup>41</sup> Frequency calculations at the same level with the same basis set were carried out to ensure that the geometries correspond to real minima. Meanwhile, geometry optimization and time dependent-DFT (TD-DFT) calculations were examined in the gas phase.<sup>42</sup> Gaussview 03 and Chemcraft software were used for visualization purposes.<sup>43</sup>

## Cell culture

Human hepatocellular carcinoma cells (HepG2) were cultured in Dulbecco's Modified Eagle's Medium (DMEM) containing 10% fetal bovine serum and 1% penicillin-streptomycin. Cells were maintained in an incubator at 37 °C in a 5% CO<sub>2</sub>/air environment.

## Cell viability assay

Cells were seeded into 96 well plates (1 × 10<sup>4</sup> cells per well per 100 μL of culture medium) and grown overnight. Cells were then treated with the vehicle (DMSO) and increasing concentrations of probes: PTCA-Cu<sup>2+</sup> (0, 1, 5, 10, 25, 50, 75, 100 μM) in a fresh medium and incubated for 24 h. Cell viability was measured using MTT (4,5-dimethylthiazol-2-yl-2,5-diphenyl-tetrazolium bromide) assay following the standard protocol.<sup>44</sup> Percent of viability was calculated relative to vehicle treated cells vs. probe treated cells.

## Cellular imaging

HepG2 cells were seeded and cultured in confocal imaging chamber slides. On confluence, cells were switched to serum free DMEM with arsenic (5 μM) and incubated for 30 min. After 30 min, a PTCA-Cu<sup>2+</sup> probe (5 μM and 10 μM) was added to the designated wells and incubated for another 30 min. Finally, cells were washed three times for 5 min each with PBS buffer. The cells were then stained with DAPI mounting medium and images were captured using confocal laser scanning microscopy upon excitation at 458 nm and collection of fluorescence signals at 600 nm.

## Synthesis of the ligand (H<sub>4</sub>PTCA)

A solution of perylene-3,4,9,10-tetracarboxylic dianhydride (1 g, 2.6 mmol) and KOH (0.85 g, 15.1 mmol) in 150 ml water was stirred at room temperature for 6 hours until the colour of the solution changed from yellow to green. The pH (~7.0) of the resultant solution was adjusted using dilute HCl. The precipitates thus obtained were filtered, washed with DI water and dried under vacuum.<sup>45a</sup> Yield: 80% (650 mg); melting point: 92–96 °C; FT-IR (KBr, ν in cm<sup>-1</sup>): 2361, 2181, 2153, 1980, 1746, 1092. <sup>1</sup>H NMR (500 MHz, water-d<sub>2</sub>): δ 8.32 (d, *J* = 7.6 Hz, 2H), 7.72 (d, *J* = 7.55 Hz, 2H); <sup>13</sup>C NMR (water-d<sub>2</sub>): δ 177.02, 137.73, 131.29, 128.43, 127.95, 127.72, 120.86; HRMS: *m/z* calculated for C<sub>24</sub>H<sub>13</sub>Na<sub>2</sub>O<sub>8</sub><sup>3+</sup> [M + H + 2Na]<sup>+</sup>: 475.3331, found 475.3319.

## Synthesis of the [PTCA-Cu<sub>2</sub>(en)<sub>4</sub>(H<sub>2</sub>O)<sub>4</sub>EtOH] complex

Ethylenediamine (2 mL) was added slowly to a suspension of H<sub>4</sub>PTCA (500 mg, 1.16 mmol) and CuNO<sub>3</sub>·3H<sub>2</sub>O (140 mg, 0.58 mmol) in H<sub>2</sub>O (8 mL) and stirred at room temperature for 30 minutes. A clear solution was obtained, which was then kept under the diffusion of ethanol as a solvent in a glass tube. Brown colour crystals of the [PTCA-Cu<sub>2</sub>(en)<sub>4</sub>(H<sub>2</sub>O)<sub>4</sub>EtOH] complex were obtained after standing for 6–7 days at room temperature.<sup>45b</sup> Yield: 72% (450 mg). FT-IR (KBr, ν in cm<sup>-1</sup>): 3061, 2890, 2771, 2360, 2181, 2157, 1967, 1716, 1589, 1355,

1091; HRMS: *m/z* calculated for C<sub>32</sub>H<sub>40</sub>Cu<sub>2</sub>LiN<sub>8</sub>O<sub>11</sub><sup>+</sup> (845.1357), C<sub>32</sub>H<sub>41</sub>Cu<sub>2</sub>LiNaN<sub>8</sub>O<sub>11</sub><sup>3+</sup> (869.1545), C<sub>34</sub>H<sub>45</sub>Cu<sub>2</sub>LiNaN<sub>8</sub>O<sub>11</sub><sup>3+</sup> (897.1858).

## Results and discussion

### Description of the solid state PTCA-Cu<sup>2+</sup> complex

Single crystals of the PTCA-Cu<sup>2+</sup> complex were grown and analysed to explain the structure and coordination environment of the copper complex. The structural parameters of the complex are given in Table S2.† The PTCA-Cu<sup>2+</sup> complex crystallized in the monoclinic *P21/c* space group. The ORTEP diagram and the perspective ball and stick view of the complex are depicted in Fig. 1 and S5, respectively.† The binuclear Cu<sup>2+</sup>-system showed a distorted octahedral geometry in which two ethylenediamine molecules satisfied the equatorial coordination sites and the axial sites were coordinated through one water molecule (H<sub>2</sub>O...Cu) and one carboxylate (C-O...Cu) unit from the perylene moiety as shown in Fig. 1b and c. Here, ethylenediamine plays a key role in the formation of the PTCA-Cu(II) complex due to its chelation through bidentate donor sites. Moreover, the strong inter- and intra-molecular H-bonds between either a coordinated or an uncoordinated carboxylic group with a water molecule (H<sub>2</sub>O) and the amine group (NH<sub>2</sub>) play a significant role in the formation of the PTCA-Cu<sup>2+</sup> complex system. Interestingly, among the four carboxylate groups of the H<sub>4</sub>PTCA moiety, only two carboxylate groups were participating in coordinating two different Cu<sup>2+</sup> units axially whereas the other two carboxylate groups remained in an uncoordinated form (Fig. S5†). The bond angle [O(1)–Cu–O(2) = 170.79°] as well as bond lengths (O(2)...Cu = 2.41 Å and O(1)...Cu = 2.55 Å) between the central copper ions and two oxygen atoms resemble the ideal octahedral geometries (Fig. 1b).<sup>45b,46</sup> In the crystal system, the perylene moiety acts as a bridge between the two Cu<sup>2+</sup> centres. In the crystal lattice, both the water molecules (axial sites) were engaged in H-bonding with the uncoordinated carboxylate oxygen atoms

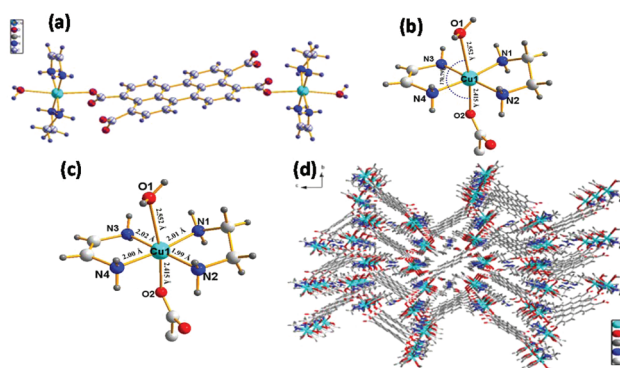


**Fig. 1** (a) ORTEP diagram of the PTCA-Cu<sup>2+</sup> complex. (b) and (c) The coordination environment of the central Cu<sup>2+</sup> ion. (d) Packing capped stick model view of PTCA-Cu<sup>2+</sup> along the a axis.

of different units (Fig. S6–S9†). Apart from the coordination sites, one uncoordinated water molecule in the crystal lattice was involved in strong H-bonding with the uncoordinated carboxylate group and NH<sub>2</sub> group of two different neighbouring units (Fig. S6†). In addition, other uncoordinated water molecules were bonded with the ethanol molecule (the nearby uncoordinated carboxylate) through O...HO (2.70 Å), OH...O (2.77 Å) and O...HO (2.80 Å) interactions, respectively (Fig. S9†). Finally, all such H-bonding interactions played an important role in forming the two-dimensional layered structure along the *a*-axis in the solid state (Fig. 1d).

### Photophysical studies

The structural analysis revealed that the synthesized PTCA–Cu<sup>2+</sup> complex contains uncoordinated carboxylate groups which can act as an anchoring group while interacting with other analytes through H-bonding. To check the photophysical properties of the developed PTCA–Cu<sup>2+</sup> complex in comparison with PTCA, UV–vis and fluorescence spectroscopy studies were performed in H<sub>2</sub>O (buffered with HEPES, 1 mM, pH = 7.2). The PTCA showed two distinct high energy absorption bands centred at 447 nm and 471 nm, respectively, and one broad low energy absorption band centred at 509 nm (Fig. S10†). These bands arose mainly due to strong  $\pi$ – $\pi^*$  and  $n$ – $\pi^*$  transitions, respectively.<sup>47</sup> Similar absorption behaviour with a decrease in absorption intensities was observed in the case of the PTCA–Cu<sup>2+</sup> complex (Fig. S10†). This envisioned the strong interaction of Cu<sup>2+</sup> with PTCA in the ground state. Meanwhile, the fluorescence behaviour of the PTCA–Cu<sup>2+</sup> complex was investigated under similar conditions. Excitation at 497 nm resulted in a very weak fluorescence signal (quantum yield ( $\Phi$ ) = 0.032) in the red region (600 nm) (Fig. S11†) due to photo-induced electron transfer (PET) from the excited perylene to Cu<sup>2+</sup>.<sup>48</sup> The paramagnetic nature of Cu<sup>2+</sup> and electron transfer (PET) from the excited perylene fluorophore to the strong electron-withdrawing Cu<sup>2+</sup> were mainly responsible for the weak fluorescence of the PTCA–Cu<sup>2+</sup> system.<sup>49–51</sup>

To check the optical response of the PTCA–Cu<sup>2+</sup> complex toward relevant analytes, both absorption and fluorescence

were recorded under similar conditions (Fig. 2 and Fig. S12†). Interestingly, no significant changes were observed in the absorption profile upon the addition of various analytes (166  $\mu$ M) such as anions (F<sup>–</sup>, Cl<sup>–</sup>, Br<sup>–</sup>, I<sup>–</sup>, N<sub>3</sub><sup>–</sup>, SO<sub>4</sub><sup>2–</sup>, AcO<sup>–</sup>, HCO<sub>3</sub><sup>–</sup>, HSO<sub>3</sub><sup>–</sup> and CN<sup>–</sup>; 1 mM) and cations (Al<sup>3+</sup>, Fe<sup>3+</sup>, Cu<sup>2+</sup>, Cd<sup>2+</sup>, Ni<sup>2+</sup>, Ag<sup>+</sup>, Mn<sup>2+</sup>, Zn<sup>2+</sup>, Na<sup>+</sup>, Mg<sup>2+</sup>, Hg<sup>2+</sup>, Co<sup>2+</sup>, Pb<sup>2+</sup>, Cr<sup>3+</sup>, and As<sup>3+</sup>; 1 mM) (Fig. S12†). But unlike other metal ions, the addition of the As<sup>5+</sup> ion (166  $\mu$ M) to the PTCA–Cu<sup>2+</sup> solution enhanced the absorption intensity (10  $\mu$ M) (Fig. S12a, S13†), which indicated strong interaction of As<sup>5+</sup> with the PTCA–Cu<sup>2+</sup> system.

Similarly, the emission profile of the PTCA–Cu<sup>2+</sup> complex system remained unaffected upon the addition of other relevant analytes (Fig. S12b†). In contrast, upon the addition of As<sup>5+</sup> a remarkable fluorescence enhancement was observed at different slit widths ( $\lambda_{\text{ex}}$  = 497 nm,  $\lambda_{\text{em}}$  = 600 nm) (Fig. S14a–d†) in the emission profile of the PTCA–Cu<sup>2+</sup> complex system with a ~900% increase in fluorescence quantum yield (quantum yield ( $\Phi$ ) = 0.344) (Fig. S14e†). It is worth mentioning that the probe also showed similar emissive properties when excited at 441 and 471 nm (Fig. S15a†). However, given that for biological studies higher wavelength excitation is preferred to reduce photon absorption, the fluorescence studies were performed at 497 nm.

The better affinity of As<sup>5+</sup> towards the PTCA–Cu<sup>2+</sup> complex system was attributed to the formation of a PTCA–As<sup>5+</sup> ensemble (Scheme 2) through chelation *via* intermolecular H-bonds between hydrogens associated with As species and ionized/non-ionized carboxyl groups of H<sub>4</sub>PTCA that led to H-bonded chelation enhanced fluorescence.<sup>30</sup> To support this phenomenon, the fluorescence behaviour of H<sub>4</sub>PTCA was examined in the presence of As<sup>5+</sup> in similar way, which displayed a slight enhancement of fluorescence signal with similar optical properties ( $\lambda_{\text{ex}}$  497 nm and  $\lambda_{\text{em}}$  600 nm) and emission profiles (Fig. S15b†). This experiment clearly revealed the affinity of H<sub>4</sub>PTCA towards As<sup>5+</sup>. Also, it established that in the presence of As<sup>5+</sup>, the PTCA–Cu<sup>2+</sup> complex undergoes decomplexation and forms a PTCA–As<sup>5+</sup> emissive integrated system.

Furthermore, HRMS analysis was performed to support the decomplexation mechanism. The HRMS analysis revealed strong peaks at *m/z* 845.0566, 869.5054 and 897.5420 which correspond to PTCA–Cu<sup>2+</sup>, as shown in Fig. S4.† Furthermore, an As<sup>5+</sup> solution (such as H<sub>2</sub>AsO<sub>4</sub><sup>–</sup>) was added to the PTCA–Cu<sup>2+</sup> complex system and stirred for five minutes.

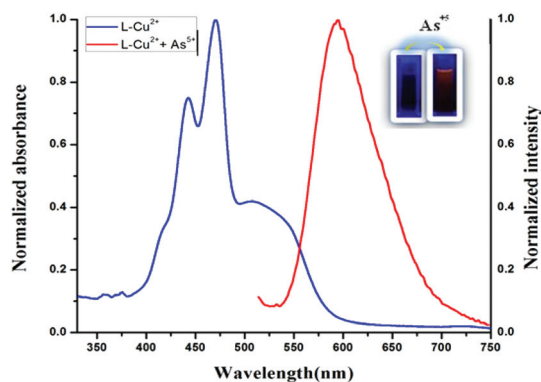
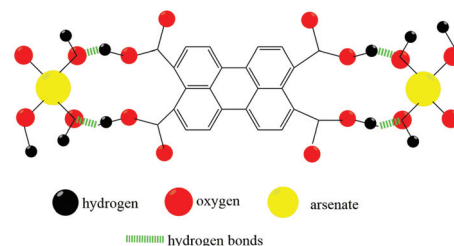


Fig. 2 The absorption and emission spectra of PTCA–Cu<sup>2+</sup> (10  $\mu$ M) upon the addition of As<sup>5+</sup> (166  $\mu$ M).



Scheme 2 Depiction of bonding in PTCA–As<sup>5+</sup>.

The resulting mixture was then subjected to HRMS analysis, which showed a strong peak at  $m/z$  713.6299, corresponding to the expected mass of the  $[\text{PTCA-2}(\text{AsH}_3\text{O}_4) + 2\text{H}^+]$  ensemble. Moreover, another strong peak at  $m/z$  257.0596 corresponding to  $[\text{Cu}(\text{en})_2(\text{CH}_3\text{CN})(\text{H}_2\text{O})_2\text{-2H}^+]$  was also observed, which indicated that Cu(II) leaves perylene carboxylate, leading to decomposition of the complex and formation of a new Cu(II) complex with ethylenediamine (Fig. S16<sup>†</sup>). These results strongly supported our proposed mechanism that the PTCA-As<sup>5+</sup> ensemble was developed upon addition of As<sup>5+</sup> to the PTCA-Cu<sup>2+</sup> system. In order to strengthen the proposed mechanism, the binding constants of PTCA-Cu<sup>2+</sup> and PTCA-As<sup>5+</sup> were calculated and found to be  $0.377 \times 10^8 \text{ M}^{-2}$  and  $8.50 \times 10^8 \text{ M}^{-2}$ , respectively. The higher binding constant of PTCA-As<sup>5+</sup> also demonstrated the disassembly process (Fig. S17–18<sup>†</sup>).<sup>52,53</sup>

Next, pH dependent studies have been carried out to investigate the sensing ability of PTCA-Cu<sup>2+</sup> towards As<sup>5+</sup> in a wider range of pH (Fig. S19<sup>†</sup>). It was observed that pH had a negligible influence on the fluorescence profile of PTCA-Cu<sup>2+</sup> upon the addition of As<sup>5+</sup>. The system is stable enough in both acidic and basic media. This may be attributed to the polyprotic nature of the As<sup>5+</sup> oxo-anion that led to different oxyanion species, H<sub>2</sub>AsO<sub>4</sub><sup>-</sup> and HAsO<sub>4</sub><sup>2-</sup> in slightly acidic and basic media, respectively. Both the oxo-anions participated in H-bonding for the formation of the PTCA-As<sup>5+</sup> ensemble.<sup>54</sup>

Furthermore, the sensitivity and selectivity of the PTCA-Cu<sup>2+</sup> complex toward As<sup>5+</sup> in the presence of various other anions were studied. The fluorescence profile of PTCA-Cu<sup>2+</sup> remained unaffected upon the addition of an excess amount of different anions except the As<sup>5+</sup> ion. Hence, these experimental outcomes strongly supported the excellent selectivity of the PTCA-Cu<sup>2+</sup> complex toward As<sup>5+</sup> as compared to other competitive analytes (Fig. 3).

To check the potential of the system, the limit of detection was calculated using  $3\sigma/\text{slope}$ .<sup>55</sup> It was found that the developed system can detect as low as 26 nM As<sup>5+</sup> (Fig. S20<sup>†</sup>). Therefore, the PTCA-Cu<sup>2+</sup> platform could be strongly recommended as a potential optical material for trace amount detection of As<sup>5+</sup> through turn-on signalling.<sup>49a</sup>

Given that arsenic contaminated water is a global concern, we explored the PTCA-Cu<sup>2+</sup> platform for the detection of the

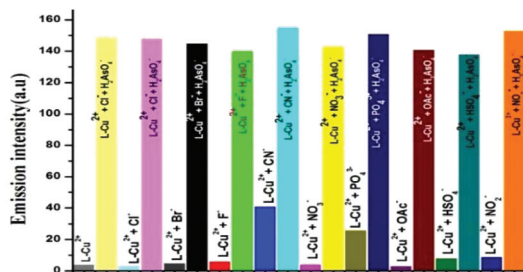


Fig. 3 Selectivity of PTCA-Cu<sup>2+</sup> (10 μM) towards As<sup>5+</sup> (166 μM) in the presence of an excess amount (332 μM) of different anions (Cl<sup>-</sup>, F<sup>-</sup>, Br<sup>-</sup>, HSO<sub>4</sub><sup>-</sup>, CN<sup>-</sup>, NO<sub>3</sub><sup>-</sup>, PO<sub>4</sub><sup>3-</sup>, ClO<sub>4</sub><sup>-</sup> and CH<sub>3</sub>COO<sup>-</sup>) in H<sub>2</sub>O buffered with HEPES (1 mM), pH = 7.2 ( $\lambda_{\text{ex}}$  497 nm and  $\lambda_{\text{em}}$  600 nm).

As<sup>5+</sup> ion in real water samples. Groundwater and river water samples were collected and filtered to remove larger particles using a 0.2 μM syringe filter. Next, different concentrations of As<sup>5+</sup> solutions were prepared using real water samples and examined through fluorescence titrations of the PTCA-Cu<sup>2+</sup> ensemble in the presence of the As<sup>5+</sup> ion in real water samples (the same method as that described above). As expected, different concentrations of As<sup>5+</sup> ions were efficiently detected using a PTCA-Cu<sup>2+</sup> ensemble (Fig. S21–S22<sup>†</sup>).

## Theoretical studies

Theoretical investigations have been performed for a better understanding of the geometry of the H<sub>4</sub>PTCA ligand and its complexation mechanism with Cu<sup>2+</sup> and As<sup>5+</sup> in the gas phase. Geometry optimizations and frontier molecular orbital calculations were carried out using LANL2DZ for the Cu<sup>2+</sup> complex and the 6-31G(d,p) basis set for C, H, O<sup>39,40</sup> of density functional theory using the Gaussian 09 suite of programs.<sup>41</sup> Single-crystal X-ray diffraction studies predicted the solid state geometry of the Cu<sup>2+</sup> complex, which was further optimized in the gaseous state to confirm whether the geometries correspond to real minima or not. Frequency calculations at the same level with the same basis set were carried out. The optimized geometry of H<sub>4</sub>PTCA is shown in Fig. S23.<sup>†</sup>

The optimized structure strongly suggests the possibility of hydrogen bonding between the -COOH proton and the carbonyl oxygen (O–H distance is 2.26 Å). The frontier molecular orbitals of H<sub>4</sub>PTCA are depicted in Fig. S24.<sup>†</sup> The HOMO and LUMOs are mainly located on the perylene ring. The HOMO–LUMO energy gap is 2.77 eV. The current probe is found to form a 1 : 2 ligand–metal complex with Cu<sup>2+</sup> in the presence of ethylenediamine in the solid state. The same was verified by mass spectra analysis in the liquid state. To support the data obtained from crystal data and mass spectral studies, theoretical studies have been carried out. From the optimized structure it is evident that the Cu<sup>2+</sup> ions coordinate with one of the carboxyl groups of the ligand (Fig. 4) in the presence of ethylenediamine. In addition, Cu<sup>2+</sup> also interacts with one water molecule. The optimized structure suggests the possibility of hydrogen bonding between the NH hydrogen and carbonyl functionality of the COOH group (O–H distance is 1.63 Å). Moreover, there is a possibility of hydrogen bonding between the -NH proton and the water molecule oxygen (O–H distance

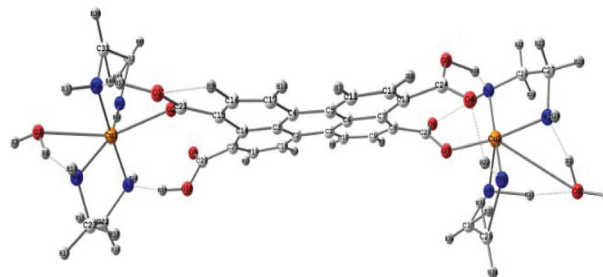


Fig. 4 Ground state optimized geometry of PTCA-Cu<sup>2+</sup>.

is 1.72 Å). The frontier molecular orbitals of the PTCA-Cu<sup>2+</sup> complex are depicted in Fig. S25.†

The HOMOs are mainly located on the perylene ring and its intimate neighbours, while the LUMOs are concentrated on one of the ethylenediamine-Cu<sup>2+</sup> ensembles of the whole complex. The HOMO-LUMO energy gap is 0.86 eV. The PTCA is found to form a 1:2 ligand-metal ensemble with As<sup>5+</sup> through intermolecular hydrogen bonding, while mass spectral studies gave strong evidence of 1:2 ligand-metal ensemble formation. To support the data obtained from mass spectral studies, theoretical studies have been carried out. From the optimized structure it is evident that the two As<sup>5+</sup> ions form an ensemble through H-bonding with the carboxyl group of the ligand (Fig. S26.†). The frontier molecular orbitals of the PTCA-As<sup>5+</sup> complex are depicted in Fig. S27.† The HOMOs mainly lie on the perylene ring and its intimate neighbours, while the LUMOs are concentrated on one of the As<sup>5+</sup> units of the whole complex. The HOMO-LUMO gap is 2.01 eV. Additionally, TD-DFT calculations have been performed to correlate theoretical absorption spectra of H<sub>4</sub>PTCA, PTCA-Cu<sup>2+</sup> and PTCA-As<sup>5+</sup> ensembles with the experimental observations. This analysis reveals absorption bands at 488.56 nm for H<sub>4</sub>PTCA, 492.07 nm, 499.84 nm for PTCA-Cu<sup>2+</sup> and 477.88 nm for the PTCA-As<sup>5+</sup> ensemble (Fig. S28, S29 and S30.†). These values are in close proximity to the experimental absorption values.

#### Imaging of intracellular arsenic with the PTCA-Cu<sup>2+</sup> probe

The highly selective binding affinities of PTCA-Cu<sup>2+</sup> towards arsenic made us interested in determining its suitability for intracellular arsenic imaging. For this purpose, 5 μM arsenic

pre-treated HepG2 cells were incubated with the PTCA-Cu<sup>2+</sup> probe (5 μM and 10 μM) for 30 min. Fig. 5 shows an observable orange fluorescence in the cytoplasm of HepG2 cells. It is noted that no detectable fluorescence is observed from the cells when HepG2 cells were incubated with the probe alone without arsenic treatment under the same imaging conditions.

These data clearly revealed that the PTCA-Cu<sup>2+</sup> was highly permeable to cells and the fluorescence intensity of the probe was reflected in the levels of cellular arsenic present in the cytoplasm.

Most important, the data illustrated in Fig. S31.† reveal that the cell viability remains more than 99% post 24 h even at a probe concentration of 20 μM (4 times higher than the concentration used for cellular imaging), implying that PTCA-Cu<sup>2+</sup> is totally safe and non-toxic up to 20 μM. These results suggest that PTCA-Cu<sup>2+</sup> can be used as a selective endogenous cellular arsenic sensor.

## Conclusions

To conclude, an organic-inorganic hybrid system based on the perylene-Cu<sup>2+</sup> complex bearing free carboxyl functionality as a mega-Stokes optical probe has been explored for the recognition of As<sup>5+</sup> in aqueous solution. To our knowledge, this the first red-emissive small molecule optical material for arsenic recognition with detection limits at the nanomolar level. It is worth mentioning that the probe is water soluble and responds well with good optical signals in aqueous solution. In addition, the background fluorescence issue was not a concern as the probe is almost non-fluorescent in nature. Because of its encouraging emissive properties, the ensemble was further explored for fluorescence imaging of As<sup>5+</sup> inside live cells. The probe was found to be cell permeable and successfully imaged As<sup>5+</sup> inside cellular milieu without any background fluorescence issue. Owing to the long range emissive nature of the perylene-As<sup>5+</sup> complex, no autofluorescence was observed from the cellular species during intracellular imaging of As<sup>5+</sup>. Also, the non-toxic nature of the present probe ensures its potential to be used for biological applications.

## Conflicts of interest

There are no conflicts to declare.

## Acknowledgements

Financial support received from the DST, India (SR/FT/CS-57/2010(G)) and IIT Mandi (IITM/SG/NRT-58) is thankfully acknowledged. We thank the Director, IIT Mandi for research facilities. The support of the Advanced Materials Research Centre (AMRC), IIT Mandi, for the sophisticated instrument facility is thankfully acknowledged. M. V thanks the CSIR, India for his fellowship.

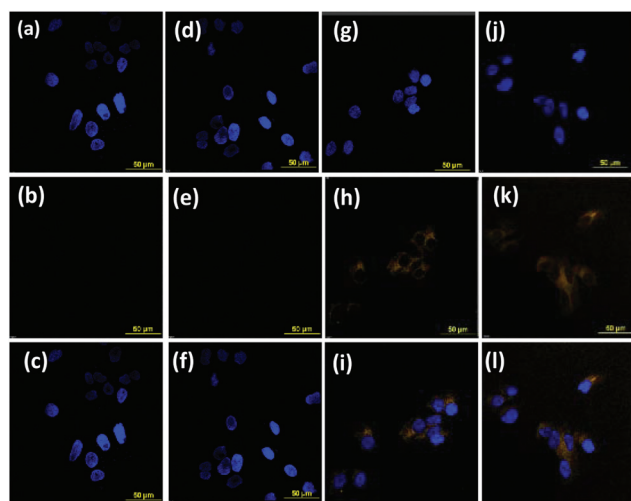


**Fig. 5** Confocal images of HepG2 cells after incubation with PTCA-Cu<sup>2+</sup> in the absence and presence of As<sup>5+</sup>. (a–c) Images with PTCA-Cu<sup>2+</sup> without As<sup>5+</sup>, (d–f) HepG2 cells were incubated with the As<sup>5+</sup> in the absence of PTCA-Cu<sup>2+</sup>, (g–i) cells were pre-treated with As<sup>5+</sup> and then incubated with the probe PTCA-Cu<sup>2+</sup> (5 μM), and (j–l) cells were pre-treated with As<sup>5+</sup> and then incubated with the probe PTCA-Cu<sup>2+</sup> (10 μM). The cell nuclei were stained with DAPI. Cell images were obtained using an excitation wavelength of 458 nm and collection of the fluorescence at 600 nm. Scale bar = 50 μm.

## Notes and references

- World Bank Water and Sanitation Program, *Towards a more effective operational response: arsenic contamination of ground water in South and East Asian countries*, 2005.
- K. Ohnishi, H. Yoshida, K. Shigeno, S. Nakamura, S. Fujisawa, K. Naito, K. Shinjo, Y. Fujita, H. Matsui, A. Takeshita, S. Sugiyama, H. Satoh, H. Terada and R. Ohno, *Ann. Intern. Med.*, 2000, **133**, 881–885.
- A. F. M. Y. Haider, M. H. Ullah, Z. H. Khan, F. Kabir and K. M. Abedin, *Opt. Laser Technol.*, 2014, **56**, 299–303.
- M. Khairy, D. K. Kampouris, R. O. Kadara and C. E. Banks, *Electroanalysis*, 2010, **22**, 2496–2501.
- (a) K. Siegfried, C. Endes, A. F. M. K. Bhuiyan, A. Kuppardt, J. Mattusch, J. R. van der Meer, A. Chatzinotas and H. Harms, *Environ. Sci. Technol.*, 2012, **46**, 3281–3287; (b) J. Das and P. Sarkar, *Environ. Sci.: Water Res. Technol.*, 2016, **2**, 693.
- E. Deliyanni, D. Bakoyannakis, A. Zouboulis and K. Matis, *Chemosphere*, 2003, **50**, 155–163.
- I. Rau, A. Gonzalo and M. Valiente, *React. Funct. Polym.*, 2003, **54**, 85–94.
- A. Banerjee, A. Sahana, S. Lohar, S. Panja, S. K. Mukhopadhyay and D. Das, *RSC Adv.*, 2014, **4**, 3887–3892.
- M. Vaclavikova, G. P. Gallios, S. Hredzak and S. Jakabsky, *Clean Technol. Environ. Policy*, 2008, **10**, 89–95.
- IARC Monogr. Eval. Carcinog. Risks Hum., 1980, **23**, 39–141.
- A. A. Ensafi, A. C. Ring and I. Fritsch, *Electroanalysis*, 2010, **22**, 1175–1185.
- P. B. Tchounwou, A. K. Patlolla and J. A. Centeno, *Toxicol. Pathol.*, 2003, **31**, 575–588.
- E. S. Hansen, *Mutat. Res.*, 1990, **239**, 163–179.
- C. J. Chen, Y. M. Hsueh, M. S. Lai, M. P. Shyu, S. Y. Chen, M. M. Wu, T. L. Kuo and T. Y. Tai, *Hypertens.*, 1995, **25**, 53–60.
- C. J. Chen, H. Y. Chiou, M. H. Chiang, L. J. Lin and T. Y. Tai, *Arterioscler., Thromb., Vasc. Biol.*, 1996, **16**, 504–510.
- M. F. Naujokas, B. Anderson, H. Ahsan, H. Vasken Aposhian, J. H. Graziano, C. Thompson and W. A. Suk, *Environ. Health Perspect.*, 2013, **121**, 3.
- H. Miao, G. Wuer and X. Shuangshuang, *Anal. Methods*, 2014, **6**, 1796.
- M. Chen, Y. Lin, C. Gu and J. Wang, *Talanta*, 2013, **104**, 53–57.
- B. Chen, W. T. Corns, P. B. Stockwell and J. H. Huang, *Anal. Methods*, 2014, **6**, 7554.
- M. A. Ferreira and A. A. Barros, *Anal. Chim. Acta*, 2002, **459**, 151–159.
- L. Chen, N. Zhou, J. Li, Z. Chen, C. Liao and J. Chen, *Analyst*, 2011, **136**, 4526.
- P. Salaün, K. B. Gibbon-Walsh, G. M. S. Alves, H. M. V. M. Soares and C. M. G. van den Berg, *Anal. Chim. Acta*, 2012, **746**, 53–62.
- K. Gibbon-Walsh, P. Salaün and C. M. G. van den Berg, *Anal. Chim. Acta*, 2012, **710**, 50–57.
- R. A. Dar, N. G. Khare, D. P. Cole, S. P. Karna, A. K. Srivastava, M. Liu and D. Wang, *RSC Adv.*, 2014, **4**, 14432.
- U. Kohlmeier, E. Jantzen, J. Kuballa and S. Jakubik, *Anal. Bioanal. Chem.*, 2003, **377**, 6–13.
- V. C. Ezeh and T. C. Harrop, *Inorg. Chem.*, 2012, **51**, 1213–1215.
- (a) S. A. Banerjee, A. Sahana, S. Panja, S. K. Mukhopadhyay and D. Das, *RSC Adv.*, 2013, **4**, 3887–3892; (b) M. Baglan and S. Atilgan, *Chem. Commun.*, 2013, **49**, 5325.
- (a) A. Sahana, A. Banerjee, S. Lohar, S. Panja, S. K. Mukhopadhyay, J. S. Matalobos and D. Das, *Chem. Commun.*, 2013, **49**, 7231–7233; (b) S. Lohar, A. Sahana, A. Banerjee, A. Banik, S. K. Mukhopadhyay and J. S. Matalobos, *Anal. Chem.*, 2013, **85**, 1778–1783.
- S. Lohar, S. Pal, B. Sen, M. Mukherjee, S. Banerjee and P. Chattopadhyay, *Anal. Chem.*, 2014, **86**, 11357–11361.
- B. Dey, R. Saha and P. Mukherjee, *Chem. Commun.*, 2013, **49**, 7064.
- B. Dey, P. Mukherjee, R. K. Mondal, A. P. Chattopadhyay, I. Hauli, S. K. Mukhopadhyay and M. Fleck, *Chem. Commun.*, 2014, **50**, 15263–15266.
- S. Lohar, A. Sahana, A. Banerjee, A. Banik, S. K. Mukhopadhyay, J. Sanmartin Matalobos and D. Das, *Anal. Chem.*, 2013, **85**, 1778–1783.
- J. C. Er, M. K. Tang, C. G. Chia, H. Liew, M. Vendrell and Y. T. Chang, *Chem. Sci.*, 2013, **4**, 2168.
- (a) K. Boonkitpatarakul, J. Wang, N. Niamnont, B. Liu, L. McDonald, Y. Pang and M. Sukwattanasinitt, *ACS Sens.*, 2016, **1**, 144–150; (b) J. Zhao, S. Ji, Y. Chen, H. Guo and P. Yanga, *Phys. Chem. Chem. Phys.*, 2012, **14**, 8803–8817.
- S. Dey, S. Sarkar, D. Maity and P. Roy, *Sens. Actuators, B*, 2017, **246**, 518–534.
- CrysalisPro Program, version 171.37.33c*, Agilent Technologies, Oxford, 2012.
- O. V. Dolomanov, L. J. Bourhis, R. J. Gildea, J. A. K. Howard and H. Puschmann, *J. Appl. Crystallogr.*, 2009, **42**, 339–341.
- G. M. Sheldrick, *Acta Crystallogr.*, 2008, **A64**, 112–122.
- A. D. Becke, *J. Chem. Phys.*, 1993, **98**, 5648.
- C. Lee, W. Yang and R. G. Parr, *Phys. Rev. B: Condens. Matter*, 1988, **37**, 785–789.
- M. J. Frisch, G. W. Trucks, H. B. Schlegel, G. E. Scuseria, M. A. Robb, J. R. Cheeseman, G. Scalmani, V. Barone, B. Mennucci, G. A. Petersson, H. Nakatsuji, M. Caricato, X. Li, H. P. Hratchian, A. F. Izmaylov, J. Bloino, G. Zheng, J. L. Sonnenberg, M. Hada, M. Ehara, K. Toyota, R. Fukuda, J. Hasegawa, M. Ishida, T. Nakajima, Y. Honda, O. Kitao, H. Nakai, T. Vreven, J. A. Montgomery Jr., J. E. Peralta, F. o. Ogliaro, M. J. Bearpark, J. Heyd, E. N. Brothers, K. N. Kudin, V. N. Staroverov, R. Kobayashi, J. Normand, K. Raghavachari, A. P. Rendell, J. C. Burant, S. S. Iyengar, J. Tomasi, M. Cossi, N. Rega, N. J. Millam, M. Klene, J. E. Knox, J. B. Cross, V. Bakken, C. Adamo, J. Jaramillo, R. Gomperts, R. E. Stratmann, O. Yazyev, A. J. Austin, R. Cammi, C. Pomelli, J. W. Ochterski, R. L. Martin,

- K. Morokuma, V. G. Zakrzewski, G. A. Voth, P. Salvador, J. J. Dannenberg, S. Dapprich, A. D. Daniels, Å. d. n. Farkas, J. B. Foresman, J. V. Ortiz, J. Cioslowski and D. J. Fox, *Gaussian 09*, in, *Gaussian, Inc*, Wallingford, CT, USA, 2009.
- 42 B. Mennucci, R. Cammi and J. Tomasi, *J. Chem. Phys.*, 1999, **110**, 6858–6870.
- 43 R. Dennington, T. Keith and J. Millam, *GaussView, Version 5*, *Semichem Inc*, Shawnee Mission, KS, 2009.
- 44 T. Mosmann, *J. Immunol. Methods*, 1983, **65**, 55–63.
- 45 (a) J. Han, Y. Zhuo, Y. Chai and R. Yuan, *Chem. Commun.*, 2014, **50**, 3367–3369; (b) Y. Suenaga, T. Kuroda-Sowa, M. Munakata and M. Maekawa, *Polyhedron*, 1998, **17**, 2207–2211.
- 46 (a) G. A. Barclay and C. H. L. Kennard, *J. Chem. Soc.*, 1961, 5244; (b) O. P. Anderson and A. B. Packard, *Inorg. Chem.*, 1980, **19**, 2123; (c) Tables of Interatomic Distances and Configuration in molecules and Ions. Spec. Publ. - *Chem. Soc. 11*; Sutton, L. E., Ed.; 1958.
- 47 (a) C. S. Abeywickrama, K. J. Wijesinghe, R. V. Stahelin and Y. Pang, *Chem. Commun.*, 2017, **53**, 5886–5889; (b) K. Bag, P. K. Sukul, D. C. Santra, A. Roy and S. Malik, *RSC Adv.*, 2016, **6**, 34027.
- 48 G. A. Crosby and J. N. Demas, *J. Phys. Chem.*, 1971, **75**, 991–1024.
- 49 (a) M. Venkateswarulu, S. Sinha, J. Mathew and R. R. Koner, *Tetrahedron Lett.*, 2013, **54**, 4683–4688; (b) A. P. de Silva, T. S. Moody and G. D. Wright, *Analyst*, 2009, **134**, 2385–2393; (c) S. A. de Silva, A. Zavaleta, D. E. Baron, O. Allam, E. V. Isidor, N. Kashimura and J. M. Percarpio, *Tetrahedron Lett.*, 1997, **38**, 2237–2240.
- 50 T. Nagano, *Proc. Jpn. Acad., Ser. B*, 2010, **86**, 837–847.
- 51 G. Dey, M. Venkateswarulu, V. Vivekananthan, A. Pramanik, V. Krishnan and R. R. Koner, *ACS Sens.*, 2016, **1**, 663–669.
- 52 M. J. Hynes, *J. Chem. Soc., Dalton Trans.*, 1993, 311–312.
- 53 S. Rochat, S. N. Steinmann, C. Corminboeuf, K. Severin, A. Villares, A. García-Lafuente, A. Ramos and J. A. Martínez, *Chem. Commun.*, 2011, **47**, 10584.
- 54 D. I. Fox, T. Pichler, D. H. Yeh and N. A. Alcantar, *Environ. Sci. Technol.*, 2012, **46**, 4553–4559.
- 55 G. L. Long and G. D. Winefordner, *Anal. Chem.*, 1983, **55**, 712A.